



CrossMark  
 click for updates

Cite this: *RSC Adv.*, 2017, 7, 5759

# Ferrocenated nanocatalysts derived from the decomposition of ferrocenium in basic solution and their aerobic activities for the rapid decolorization of methylene blue and the facile oxidation of phenylboronic acid†

Nuttapong Kumpan,<sup>a</sup> Thinnaphat Poonsawat,<sup>a</sup> Laksamee Chaicharoenwimolkul,<sup>b</sup> Soraya Pornsuwan<sup>a</sup> and Ekasith Somsook<sup>\*a</sup>

Received 20th October 2016  
 Accepted 16th December 2016

DOI: 10.1039/c6ra25515a

[www.rsc.org/advances](http://www.rsc.org/advances)

A strategic preparation of ferrocenated compounds as aerobic catalysts was successfully carried out for the decolorization of methylene blue and oxidation of phenylboronic acid without light irradiation and excess addition of hydrogen peroxide. Cyclopentadienyl radical formed by the decomposition of ferrocenium under basic conditions plays a major role in the production of reactive oxygen species (ROS) under an aerobic atmosphere.

The development of a sustainable method for applications related to reactive oxygen species (ROS) has attracted significant attention in laboratory experiments.<sup>1</sup> Singlet oxygen, superoxide, hydrogen peroxide, and hydroxyl radicals<sup>2</sup> are a group of ROS. In the past decade, the most extensive studies in the generation of ROS were mainly focused on the well-known Fenton reaction involving iron(II), hydrogen peroxide,<sup>3</sup> photocatalysts,<sup>4–8</sup> and transition metal catalysts.<sup>9,10</sup>

Iron oxide is naturally abundant and thermally stable.<sup>11,12</sup> Iron ions are widely used in the production of ROS<sup>2,13–16</sup> and their potential applications include the degradation of dyes<sup>17–20</sup> and advanced organic oxidation.<sup>21</sup> Recently, ferrocene derivatives<sup>22–28</sup> have gained the attention of our group. We are interested in the properties of ferrocenated iron oxide nanocatalysts prepared by the coprecipitation of Fe(II), Fe(III), redox active species of ferrocene ((C<sub>5</sub>H<sub>5</sub>)<sub>2</sub>Fe or Fc), and ferrocenium ((C<sub>5</sub>H<sub>5</sub>)<sub>2</sub>FeH<sup>+</sup> or Fc<sup>+</sup>) under basic conditions.<sup>29</sup> The nanocatalysts could completely remove methylene blue in the absence of light and hydrogen peroxide within 2 hours and could be reused 12 times using sodium chloride solution as a reactivator. The production of active species may be proposed as cyclopentadienyl radicals derived from the

demetallation of ferrocenium. The initial degradation mechanism of ferrocenium derivatives in the presence of a nucleophilic solvent has been previously reported.<sup>25,30,31</sup>

To the best of our knowledge, there are no reports that propose the generation of ROS from cyclopentadienyl radicals for the oxidation of phenylboronic acid. It should be emphasized that a radical initiator is not required for the generation of cyclopentadienyl radicals in the ferrocenated compounds. Moreover, the ferrocenated compounds in this study were generated from ferrocene only without the coprecipitation with other iron ions. Cyclopentadienyl radicals in ferrocenated compounds were still active even though the prepared sample had been left under a regular atmosphere for a period of time. Herein, we show the rapid activity of ferrocenated compounds on the decolorization of methylene blue with other reactivators (NaCl, NaI, water, and seawater), as well as the efficient transformation of phenylboronic acid to phenol under an aerobic atmosphere.

First, ferrocenated compounds were generated from ferrocene in concentrated sulfuric acid to yield ferrocenium (Fc<sup>+</sup>) species appearing as a blue viscous solution,<sup>32,33</sup> and then an orange precipitate was produced in the solution by adjusting the pH value to 12 with sodium hydroxide (Fig. S1, ESI†). The possible theoretical compositions of the ferrocenated compounds consisted of iron oxide, ferrocene, and cyclopentadienyl radical, as shown in Scheme 1.

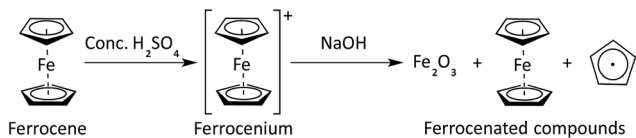
The particle size of the prepared ferrocenated compounds was in the range of nanoscale, as shown in the TEM images (Fig. S2, ESI†). It also has the structure similar to commercial ferrocene, as illustrated in the XRD pattern (Fig. S3, ESI†). Some residue of Fe<sub>3</sub>O<sub>4</sub> was confirmed by DSC/TGA curve (Fig. S4, ESI†). The temperature at 714 °C and the mass loss of about 10% corresponded to the phase transition from Fe<sub>3</sub>O<sub>4</sub> to FeO,

<sup>a</sup>NANOCAST Laboratory, Center for Catalysis Science and Technology (CAST), Department of Chemistry and Center of Excellence for Innovation in Chemistry, Faculty of Science, Mahidol University, 272 Rama VI Rd., Ratchathewi, Bangkok 10400, Thailand. E-mail: [ekasith.som@mahidol.ac.th](mailto:ekasith.som@mahidol.ac.th); Fax: +66 23547151; Tel: +66 22015123

<sup>b</sup>Chemistry Division, Faculty of Science and Technology, Suratthani Rajabhat University, 272 Moo 9, Surat-Nasan Rd., Khuntale, Muang, Surat Thani 84100, Thailand

† Electronic supplementary information (ESI) available. See DOI: 10.1039/c6ra25515a





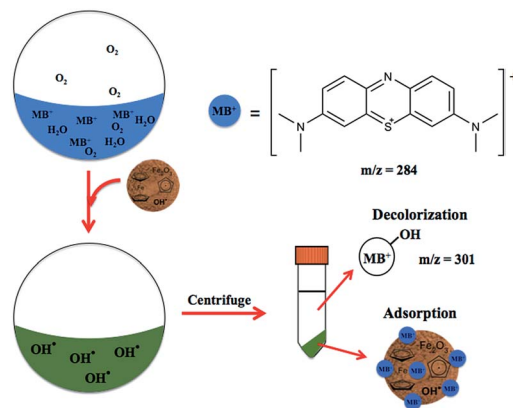
Scheme 1 The decomposition of ferrocenium species in the presence of sodium hydroxide to yield the ferrocenated compounds.

which is thermodynamically more stable at a temperature of 570 °C.<sup>34</sup> The surface area, pore-size distribution, and pore volume were determined by nitrogen adsorption/desorption isotherm analysis (−196 °C) collecting at the relative pressure ( $P/P_0$ ) range from 0.05 to 1.0. The average pore diameter was 11.16 nm and the pore volume was 0.14 cm<sup>3</sup> g<sup>−1</sup> (Fig. S5, ESI†). The corresponding BET plot showed that the surface area of the ferrocenated compounds was 49.11 m<sup>2</sup> g<sup>−1</sup>.

X-ray photoelectron spectroscopy (XPS) was used to determine the state and composition of the ferrocenated compound surface (Fig. S6 and Table S1, ESI†). The XPS spectra revealed that the binding energies of C 1s were 285.0 eV (C–C in Cp), 287.0 eV (C–O), and 288.7 eV (O–C–C), and those of O 1s were 531.4 eV (Fe–O), 532.6 eV (C–O), and 533.7 eV (O–H). The binding energies of Fe 2p at 707.2 and 708.2 eV were assigned to the pattern of Fe<sup>2+</sup> (ferrocene) and Fe<sub>3</sub>O<sub>4</sub>, respectively.<sup>35</sup> Furthermore, the binding energies of Fe<sup>3+</sup> 2p<sub>3/2</sub> were 710.1, 711.6, 713.2, and 714.6 eV.<sup>36</sup> The zeta potential value on the surface of the catalyst was −24.7 mV (Fig. S7, ESI†). Note that the surface of the catalyst was negatively charged.

Ferrocenated compounds were investigated for the production of ROS in the aqueous medium.<sup>37</sup> The hydroxyl and superoxide radical intermediates were trapped with 5,5-dimethyl-1-pyrroline-*N*-oxide (DMPO) in phosphate buffer solution (pH 7.4) and were observed by electron spin resonance (ESR), as shown in Fig. S8 and Table S2, ESI.† Cyclopentadienyl radical is proposed as a major candidate to initiate the formation of ROS under aerobic atmosphere. Unfortunately, cyclopentadienyl was not observed in ESI-MS. Instead, the  $m/z$  of 130 for dihydrofulvalene was obtained (Fig. S9, ESI†). The decolorization of methylene blue was performed using 100 mg of catalyst. The kinetic study was performed by collecting a sample (3 cm<sup>3</sup>) every 10 minutes for 2 hours. It was found that the  $C/C_0$  quickly decreased to 0.019 in 10 minutes (Fig. S11, ESI†). The possible mechanism was proposed through decolorization from the reaction of ROS with methylene blue and the adsorption on the surface of the negatively charged catalyst, as shown in Scheme 2. Moreover, the pH measurements of the reaction were carried out. The color change of methylene blue was due to the activity of the catalyst and not due to the pH change of the solution (Fig. S11, ESI†).

As shown in Fig. 1, the adsorption of methylene blue was observed by FT-IR during the first cycle of the catalysis reaction and the reactivated ferrocenated compounds exhibited the dominant peak corresponding to the C=C stretching of methylene blue at 1600 cm<sup>−1</sup>. Interestingly, the adsorbed methylene blue on the surface of ferrocenated compounds was removed by washing with salt solutions. The reusability of the ferrocenated



Scheme 2 The possible mechanism of decolorization of methylene blue in the presence of ferrocenated compounds.

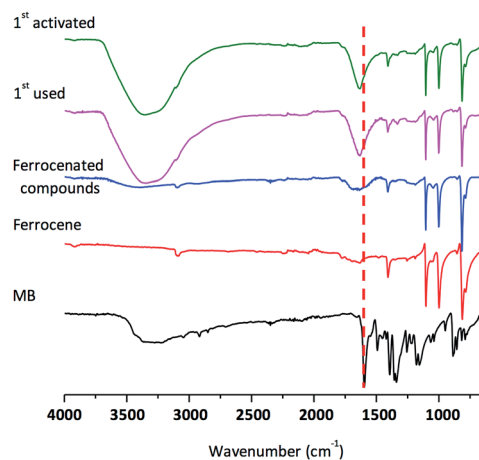


Fig. 1 FT-IR spectra of methylene blue, ferrocene, ferrocenated compounds, 1<sup>st</sup> used sample, and 1<sup>st</sup> sample activated with seawater.

compounds was achieved by reactivating with 0.1 mol dm<sup>−3</sup> NaCl, 0.1 mol dm<sup>−3</sup> NaI, and seawater and washing with DI water, as shown in Fig. 2. Moreover, the concentration of methylene blue after reactivation by ion sources is shown in Fig. S12, ESI.† The reusability of the catalyst was studied for 12 cycles. After the end of each cycle, the catalyst was reactivated for 10 minutes before using it in the next cycle. The adsorption was quite consistent (95–98%) for 8 cycles (reactivated with NaCl, and NaI and washed with DI water) and an exponential drop in the catalyst performance started from 8<sup>th</sup> cycle onwards (20–55%). In the case of reactivation by seawater, the activity of catalyst directly decreased from 97% to 77%. The used ferrocenated compounds were reactivated by salt solutions and seawater *via* an ion-exchange mechanism.

To further illustrate the catalytic activity of the ferrocenated compounds in the oxidation of phenylboronic acid towards the cyclopentadienyl radical as active species, a reaction composed of 20 mg of catalyst obtained a phenol with 14% conversion at 80 °C for 24 hours (entry 1). K<sub>2</sub>CO<sub>3</sub> was used as a base to enhance the solubility of phenylboronic acid in the phenyl boronate. Furthermore, different amounts of ferrocenated



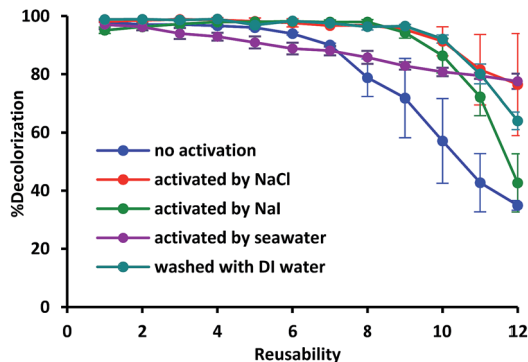


Fig. 2 Reusability of the ferrocenated catalyst with and without reactivation by NaCl, NaI, and seawater and washing by DI water.

compounds were added as catalysts in the oxidation of phenylboronic acid (entry 2, 3, 5, and 6). The results showed that the reaction conversion was increased on increasing the amount of the catalyst. The amount of ferrocenated compounds at 200 mg exhibited the best conversion yield (94%), as shown in entry 6 of Table 1. To study the effect of temperature, we attempted to lower the temperature to 31 °C and it turned out that the reaction did not proceed after 24 hours (entry 4). It was observed that higher temperature was required for this reaction. HCl was used to quench the reaction to generate phenol for the analysis of products. Biphenyl was not detected as a product, indicating that the homocoupling of phenylboronic acid did not proceed. Furthermore, the reaction was totally incomplete in the presence of FeCl<sub>2</sub>, FeCl<sub>3</sub>, ferrocene, and Fe<sub>2</sub>O<sub>3</sub> under the same conditions (entry 7–8). In the presence of an extra oxidant and in the absence of light, no significant enhancement by ferrocene and Fe<sub>2</sub>O<sub>3</sub> in the oxidation of phenylboronic acid was observed (Table S3†).

To determine whether cyclopentadienyl radicals were active species for generating ROS, the reaction was proceeded by adding distilled cyclopentadiene (0.25 mmol) and AIBN (0.125 mmol) as a radical initiator. First, the reaction in the presence of either cyclopentadiene or AIBN showed 1% and 4% yield,

Table 1 Oxidation of phenylboronic acid catalyzed by the ferrocenated compounds through cyclopentadienyl radical as active species<sup>a</sup>

Entry	Catalyst	Conversion <sup>b</sup> (%)
1	Ferrocenated compounds (20 mg)	14
2	Ferrocenated compounds (50 mg)	36
3	Ferrocenated compounds (100 mg)	50
4 <sup>c</sup>	Ferrocenated compounds (150 mg)	1
5	Ferrocenated compounds (150 mg)	91
6	Ferrocenated compounds (200 mg)	94
7	FeCl <sub>2</sub>	0
8	FeCl <sub>3</sub>	0
9	Ferrocene (100 mg)	1
10	Fe <sub>2</sub> O <sub>3</sub> (100 mg)	4

<sup>a</sup> Reaction conditions: phenylboronic acid (0.25 mmol), K<sub>2</sub>CO<sub>3</sub> (300 mol%), and H<sub>2</sub>O (10 cm<sup>3</sup>) under aerobic atmosphere at 80 °C. <sup>b</sup> % conversion of phenylboronic acid to phenol analyzed by GC-MS with hexadecane as the internal standard. <sup>c</sup> Reaction at 31 °C.

Table 2 The oxidation of phenyl boronic acid in the presence of cyclopentadiene and azobisisobutyronitrile (AIBN)<sup>a</sup>

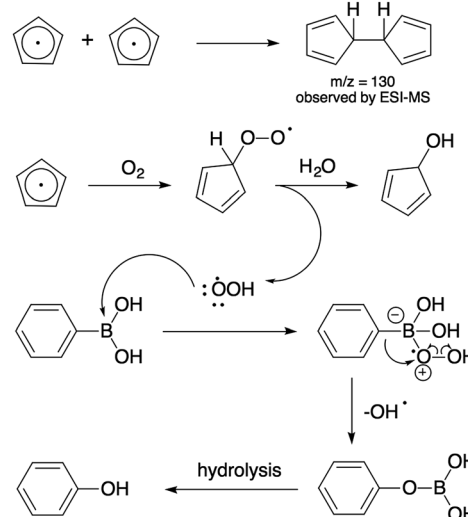
Entry	Catalyst	Yield <sup>b</sup> (%)
1	Cyclopentadiene (0.25 mmol)	1
2	Azobisisobutyronitrile (0.125 mmol)	4
3	Cyclopentadiene (0.25 mmol) and azobisisobutyronitrile (0.125 mmol)	98

<sup>a</sup> Reaction conditions: phenylboronic acid (0.25 mmol), THF : H<sub>2</sub>O (1 : 1) 5 cm<sup>3</sup>, for 24 hours under an aerobic atmosphere at 80 °C. <sup>b</sup> % yield of phenylboronic acid to phenol analyzed by GC-MS with hexadecane as the internal standard.

respectively (entry 1 and 2 in Table 2). The results indicated high performance of the cyclopentadienyl radicals with 98% yield under atmospheric oxygen at 80 °C, as shown in Table 2 (entry 3). This confirms that cyclopentadienyl radicals play a major role as the active species in the oxidation of phenylboronic acid.

Due to the low activity of ferrocene and iron oxide, the aerobic oxidation might be driven by the plausible mechanism of reactive oxygen species generated from the cyclopentadienyl radicals in the ferrocenated compounds with dioxygen. We, therefore, propose that the oxidation of phenylboronic acid occurs through the generation of perhydroxyl radical, and then generates phenol as the product. The radical is generated from the fast disproportionation of superoxide radical in water, as shown in Scheme 3.

In summary, ferrocenated compounds were successfully synthesized without coprecipitation with other iron species. This catalyst provides a good performance in the decolorization of methylene blue and oxidation of phenylboronic acid through ROS. Cyclopentadienyl radical play a key role in the generation of hydroxyl and superoxide radicals. The development of the applications of ferrocenated compounds will be further investigated in the future.



Scheme 3 Proposed mechanism for the aerobic oxidation of phenylboronic acid through perhydroxyl radical.



## Experimental sections

### Materials

All chemicals including ferrocene (ACROS), sulfuric acid (RCI Labscan), sodium chloride (Fisher Chemical), sodium iodide (Merck), sodium hydroxide (Merck), 5,5-dimethyl-1-pyrroline-*N*-oxide (DMPO, Aldrich), monosodium phosphate (RCI Labscan), disodium phosphate (Aldrich), methylene blue (Merck), phenylboronic acid (ACROS), potassium carbonate (Carlo Erba), cyclopentadiene (Aldrich), tetrahydrofuran (THF, RCI Labscan), and azobisisobutyronitrile (AIBN, Aldrich) were of analytical grade and used as received without further purification. Deionized water ( $R \geq 18.2 \text{ M}\Omega \text{ cm}$ ) was obtained from Nanopure® Analytical Deionization Water. Seawater was filtered as achieved (2<sup>nd</sup> June, 2014) from Nangkham beach, Don Sak district, Surat Thani, Thailand.

### Instruments

The ferrocenated compounds were characterized *via* X-ray powder diffraction (XRD) using a Bruker D8 ADVANCE diffractometer with Cu-K $\alpha$  radiation between 10° and 80° (2 theta). The results of TEM measurement were obtained using a Tecnai G2 Sphera transmission electron microscope operated at 80 kV. Fourier transform-infrared spectroscopy (FT-IR) was performed using Bruker Hong Kong Limited model ALPHA. The UV-visible spectrophotometer was a UV-2600 SHIMADZU operated in range of 200–800 nm. Thermogravimetric analysis (DSC/TGA) was performed using a TA instruments SDT2960 simultaneous at the heating rate of 20 °C per minute in the range from room temperature to 800 °C under nitrogen gas. Electrospray ionization (ESI) mass spectrometry was carried out using a microTOF and in the positive mode ion. Electron paramagnetic resonance spectroscopy (EPR) was carried out using JEOL JES-RE2X operated in the X-band microwave (8.8–9.6 GHz), magnetic field range of 3.1 T, cylindrical cavity resonator (TE011 mode), and with the program ES-PRIT. X-ray photoelectron spectroscopy (XPS) was performed using a Kratos Axis Ultra. The surface area, pore size, and pore volume were determined by Brunauer–Emmett–Teller (BET) method using a Quantachrome Autosorb Automated Gas Sorption System with nitrogen adsorption. The zeta potentials were determined using a Zetasizer Nano-ZS model ZEN 3600. Gas chromatography with mass spectrometry (GC-MS) spectra were obtained by Agilent 7890 (GC) and Agilent 5975 (MS) with an HP-5 capillary column.

### Preparation of the ferrocenated compounds

Ferrocene (30 mmol, 5.58 g) was added to concentrated sulfuric acid (2 cm<sup>3</sup>) and stirred to be a dark blue mixture. Then, water (5 cm<sup>3</sup>) was added and the mixture was stirred for 30 minutes. The mixture turned to an orange precipitate by adjusting the pH value to 12 with 2 mol dm<sup>-3</sup> NaOH and allowed to stir at room temperature for 1 hour. The precipitate was collected by centrifugation at 4500 rpm for 10 minutes and washed with DI water until a clear solution was obtained. The catalyst was dried overnight at 100 °C.

### Decolorization of methylene blue

The ferrocenated compounds (0.10 g) were added into the methylene blue solution ( $1 \times 10^{-5} \text{ mol dm}^{-3}$ , 100 cm<sup>3</sup>). The reaction was continuously stirred and wrapped in aluminium foil to maintain dark conditions. The solution (3 cm<sup>3</sup>) was kinetically collected every 10 minutes for 2 hours and the catalysts were separated by centrifugation at 3300 rpm for 10 minutes. The clear supernatant was analyzed by a UV-visible spectrophotometer at  $\lambda_{\text{max}}$  664 nm. The reusability of catalyst was studied using reactivated catalyst.

### Reactivation of the catalyst

After the process was completed, the used catalyst was separated by centrifugation at 3300 rpm for 10 minutes and activated by stirring in 100 cm<sup>3</sup> of reactivators (0.1 mol dm<sup>-3</sup> NaCl, 0.1 mol dm<sup>-3</sup> NaI, seawater and DI water) for 10 minutes. The reactivated catalyst was separated by centrifugation at 3300 rpm for 10 minutes and started the next run without drying.

### General oxidation condition of phenylboronic acid

Phenylboronic acid (0.25 mmol) and potassium carbonate (0.75 mmol) were dissolved in DI water (10 cm<sup>3</sup>). The catalyst was added into the solution and stirred at the desired temperatures for 24 hours. The reaction was quenched with 1 mol dm<sup>-3</sup> HCl and the catalyst was separated out. The product was extracted with ethylacetate and analyzed using GC-MS with hexadecane as the internal standard.

## Acknowledgements

The financial support received from the Biofuel development for Thailand fund through the Center of Excellence for Innovation in Chemistry (PERCH-CIC), Royal Golden Jubilee Ph.D. Program (Grant No. PHD/0271/2550) to the PhD student 3.II.MU/50/A.4 and Development and Promotion of Science and Technology Talents Project (DPST) is acknowledged.

## Notes and references

- 1 C. D. Georgiou, H. J. Sun, C. P. McKay, K. Grintzalis, I. Papapostolou, D. Zisimopoulos, K. Panagiotidis, G. S. Zhang, E. Koutsopoulou, G. E. Christidis and I. Margiolaki, *Nat. Commun.*, 2015, **6**, 1–11.
- 2 H. H. Wu, J. J. Yin, W. G. Wamer, M. Y. Zeng and Y. M. Lo, *J. Food Drug Anal.*, 2014, **22**, 86–94.
- 3 A. Dhakshinamoorthy, S. Navalon, M. Alvaro and H. Garcia, *ChemSusChem*, 2012, **5**, 46–64.
- 4 W. W. He, H. K. Kim, W. G. Warner, D. Melka, J. H. Callahan and J. J. Yin, *J. Am. Chem. Soc.*, 2014, **136**, 750–757.
- 5 N. Waiskopf, Y. Ben-Shahar, M. Galchenko, I. Carmel, G. Moshitzky, H. Soreq and U. Banin, *Nano Lett.*, 2016, **16**, 4266–4273.
- 6 Y. Q. Zou, J. R. Chen, X. P. Liu, L. Q. Lu, R. L. Davis, K. A. Jorgensen and W. J. Xiao, *Angew. Chem., Int. Ed.*, 2012, **51**, 784–788.



- 7 S. P. Pitre, C. D. McTiernan, H. Ismaili and J. C. Scaiano, *J. Am. Chem. Soc.*, 2013, **135**, 13286–13289.
- 8 X. J. Lang, X. D. Chen and J. C. Zhao, *Chem. Soc. Rev.*, 2014, **43**, 473–486.
- 9 E. Vidrio, H. Jung and C. Anastasio, *Atmos. Environ.*, 2008, **42**, 4369–4379.
- 10 J. C. Ball, A. M. Straccia, W. C. Young and A. E. Aust, *J. Air Waste Manage. Assoc.*, 2000, **50**, 1897–1903.
- 11 R. M. Cornell and U. Schwertmann, *The Iron Oxides: Structure, Properties, Reactions, Occurrences and Uses*, Wiley-VCH Verlag GmbH & Co. KGaA, Weinheim, 2nd edn, 2003.
- 12 B. I. Kharisov, H. V. R. Dias, O. V. Kharissova, V. M. Jimenez-Perez, B. O. Perez and B. M. Flores, *RSC Adv.*, 2012, **2**, 9325–9358.
- 13 Y. Mizutani, S. Hashimoto, Y. Tatsuno and T. Kitagawa, *J. Am. Chem. Soc.*, 1990, **112**, 6809–6814.
- 14 S. S. Lin and M. D. Gurol, *Environ. Sci. Technol.*, 1998, **32**, 1417–1423.
- 15 A. L. T. Pham, C. Lee, F. M. Doyle and D. L. Sedlak, *Environ. Sci. Technol.*, 2009, **43**, 8930–8935.
- 16 R. J. Watts, M. K. Foget, S. H. Kong and A. L. Teel, *J. Hazard. Mater.*, 1999, **69**, 229–243.
- 17 Y. Wang, R. Priambodo, H. Zhang and Y. H. Huang, *RSC Adv.*, 2015, **5**, 45276–45283.
- 18 H. Wang and Y. M. Huang, *J. Hazard. Mater.*, 2011, **191**, 163–169.
- 19 Q. Wang, S. L. Tian and P. Ning, *Ind. Eng. Chem. Res.*, 2014, **53**, 6334–6340.
- 20 Q. Wang, S. L. Tian, J. Cun and P. Ning, *Desalin. Water Treat.*, 2013, **51**, 5821–5830.
- 21 G. Zelmanov and R. Semiat, *Water Res.*, 2008, **42**, 492–498.
- 22 P. Audebert, S. Sadki, F. Miomandre, G. Lanneau, R. Frantz and J. O. Durand, *J. Mater. Chem.*, 2002, **12**, 1099–1102.
- 23 D. Astruc, *Eur. J. Inorg. Chem.*, 2016, **2017**, 6–29.
- 24 N. Li, P. X. Zhao, M. E. Igartua, A. Rapakousiou, L. Salmon, S. Moya, J. Ruiz and D. Astruc, *Inorg. Chem.*, 2014, **53**, 11802–11808.
- 25 J. P. Hurvois and C. Moinet, *J. Organomet. Chem.*, 2005, **690**, 1829–1839.
- 26 C. Tonhauser, A. Alkan, M. Schomer, C. Dingels, S. Ritz, V. Mailander, H. Frey and F. R. Wurm, *Macromolecules*, 2013, **46**, 647–655.
- 27 D. R. Burri, I. R. Shaikh, K. M. Choi and S. E. Park, *Catal. Commun.*, 2007, **8**, 731–735.
- 28 K. Fujimura, M. Ouchi and M. Sawamoto, *ACS Macro Lett.*, 2012, **1**, 321–323.
- 29 A. Jinasan, T. Poonsawat, L. Chaicharoenwimolkul, S. Pornsuwan and E. Somsook, *RSC Adv.*, 2015, **5**, 31324–31328.
- 30 R. Prins, A. R. Korswagen and A. G. T. G. Kortbeek, *J. Organomet. Chem.*, 1972, **39**, 335–344.
- 31 G. Tabbi, C. Cassino, G. Cavigiolio, D. Colangelo, A. Ghiglia, I. Viano and D. Osella, *J. Med. Chem.*, 2002, **45**, 5786–5796.
- 32 L. Chaicharoenwimolkul, S. Chairam, M. Namkajorn, A. Khamthip, C. Kamonsatikul, U. Tewasekson, S. Jindabot, W. Pon-On and E. Somsook, *J. Appl. Polym. Sci.*, 2013, **130**, 1489–1497.
- 33 S. Chairam, W. Sriraksa, M. Amatongchai and E. Somsook, *Sensors*, 2011, **11**, 10166–10179.
- 34 S. Y. Zhao, D. K. Lee, C. W. Kim, R. G. Cha, Y. H. Kim and Y. S. Kang, *Bull. Korean Chem. Soc.*, 2006, **27**, 237–242.
- 35 A. W. Taylor and P. Licence, *ChemPhysChem*, 2012, **13**, 1917–1926.
- 36 A. P. Grosvenor, B. A. Kobe, M. C. Biesinger and N. S. McIntyre, *Surf. Interface Anal.*, 2004, **36**, 1564–1574.
- 37 M. A. Voinov, J. O. S. Pagan, E. Morrison, T. I. Smirnova and A. I. Smirnov, *J. Am. Chem. Soc.*, 2011, **133**, 35–41.

